molecules

MDPI

Communication

Calcium Sulfite Solids Activated by Iron for Enhancing As(III) Oxidation in Water

Minjuan Cai [1], Sen Quan [1,2,*], Jinjun Li [1], Feng Wu [1] and Gilles Mailhot [3]

[1] Hubei Key Lab of Biomass Resource Chemistry and Environmental Biotechnology, School of Resources and Environmental Science, Wuhan University, Wuhan 430079, China; caiminjuan@whu.edu.cn (M.C.); lijinjun@whu.edu.cn (J.L.); fengwu@whu.edu.cn (F.W.)
[2] Hubei Academy of Environmental Science, Wuhan 430072, China
[3] CNRS, SIGMA Clermont, Institut de Chimie de Clermont-Ferrand, Université Clermont Auvergne, F-63000 Clermont–Ferrand, France; gilles.mailhot@uca.fr
* Correspondence: quansen@whu.edu.cn

Abstract: Desulfurized gypsum (DG) as a soil modifier imparts it with bulk solid sulfite. The Fe(III)–sulfite process in the liquid phase has shown great potential for the rapid removal of As(III), but the performance and mechanism of this process using DG as a sulfite source in aqueous solution remains unclear. In this work, employing solid $CaSO_3$ as a source of SO_3^{2-}, we have studied the effects of different conditions (e.g., pH, Fe dosage, sulfite dosage) on As(III) oxidation in the Fe(III)–$CaSO_3$ system. The results show that 72.1% of As(III) was removed from solution by centrifugal treatment for 60 min at near-neutral pH. Quenching experiments have indicated that oxidation efficiencies of As(III) are due at 67.5% to $HO^{\bullet}$, 17.5% to $SO_5^{\bullet-}$ and 15% to $SO_4^{\bullet-}$. This finding may have promising implications in developing a new cost-effective technology for the treatment of arsenic-containing water using DG.

Keywords: desulfurized gypsum; Fe(III); $CaSO_3$; As(III); resource utilization

Citation: Cai, M.; Quan, S.; Li, J.; Wu, F.; Mailhot, G. Calcium Sulfite Solids Activated by Iron for Enhancing As(III) Oxidation in Water. *Molecules* **2021**, *26*, 1154. https://doi.org/10.3390/molecules26041154

Academic Editor: Fernando J. Beltrán Novillo

Received: 30 January 2021
Accepted: 19 February 2021
Published: 21 February 2021

1. Introduction

The wet desulfurization process has significant advantages of fast reaction and high efficiency, and has been widely used in China. However, desulfurized gypsum (DG) cannot be fully utilized, and its disposal constitutes a waste of resources [1,2]. Currently, DG is mainly used as a soil conditioner [3], serving to improve certain properties of soil, such as its pH, water absorption, water retention, and so on. The potential oxidative ability of DG towards heavy metals or organic pollutants in soil-containing transition metals has rarely been reported [4–7].

Recently, several investigations have shown that sulfate radical ($SO_4^{\bullet-}$)-based advanced oxidation processes work well for the removal of organic and inorganic pollutants in groundwater and wastewater treatment [8–10]. The commonly used oxidants include persulfate (PS), peroxymonosulfate (PMS), and sulfite. Compared to PS and PMS, sulfite has significant advantages of low toxicity, low cost, and easy preparation, thus making it both environmentally friendly and economic [11]. Transition metal systems, such as Fe(II/III), have been reported to activate sulfite, such that it has a good oxidation effect on arsenic and organic pollutants in water [12–16]. Additionally, iron-based nanomaterials of high superficial activity also had a good effect on removing heavy metal pollutants in the environment [17,18]. In the Fe(II/III)-sulfite system, S(IV) can be catalytically oxidized under certain conditions to produce a series of oxysulfur species, including sulfite radical ($SO_3^{\bullet-}$) and sulfate radical ($SO_4^{\bullet-}$) [19–21]. An intrinsic mechanism has been proposed for this system, which includes the following reactions (Equations (1)–(8)) [22–26]:

$$Fe^{2+} + HSO_3^- \rightleftharpoons FeHSO_3^+ \text{ (rapid equilibration)} \quad (1)$$

$$4FeHSO_3^+ + O_2 \rightarrow 4FeSO_3^+ + 2H_2O \quad (2)$$

$$FeSO_3^+ \rightarrow Fe^{2+} + SO_3^{\bullet-} \ (k_f = 0.19\ s^{-1}) \quad (3)$$

$$SO_3^{\bullet-} + O_2 \rightarrow SO_5^{\bullet-} \ (k_4 < 10^9\ mol^{-1}\ L\ s^{-1}) \quad (4)$$

$$SO_5^{\bullet-} + HSO_3^- \rightarrow SO_3^{\bullet-} + HSO_5^- \ (k_5 = (10^4\text{-}10^7)\ mol^{-1}\ L\ s^{-1}) \quad (5)$$

$$Fe^{2+} + HSO_5^- \rightarrow SO_4^{\bullet-} + Fe^{3+} + OH^- \ (k_6 = (10^4\text{-}10^7)\ mol^{-1}\ L\ s^{-1}) \quad (6)$$

$$Fe^{3+} + HSO_3^- \rightleftharpoons FeSO_3^+ + H^+ \ (\log k_7 = 2.45) \quad (7)$$

$$SO_5^{\bullet-} + HSO_3^- \rightarrow SO_4^{2-} + SO_4^{\bullet-} + H^+ \ (k_8 = (10^4\text{-}10^7)\ mol^{-1}\ L\ s^{-1}) \quad (8)$$

In actual application processes, soluble SO_3^{2-} is consumed very rapidly. Due to the slow dissolution of solid $CaSO_3$, the concentration of soluble SO_3^{2-} in the solution can keep in an appropriate range [27]. Although Fe(II) activated homogeneous sulfite has been fully studied and reported, the activation mechanism of heterogeneous calcium sulfite remains unclear. In summary, it was necessary to research and develop new utilization methods of calcium sulfite waste.

In this work, $CaSO_3$ has been directly employed as a sulfite donor to assess the oxidation capability of the Fe(III)–sulfite system. The effects of $CaSO_3$/Fe(III) concentration, pH, and initial concentrations of As(III) have been investigated. Free radical quenching experiments were then performed to determine the contributions of reactive species in this system. Our work may contribute to an understanding of the main mechanisms of As(III) removal using the iron–$CaSO_3$ system and provide a theoretical basis for the use of desulfurized gypsum as a soil conditioner.

2. Results and Discussion

2.1. Control Experiments

As shown in Figure 1, As(tot) remained unchanged in both the control experiments and the Fe(III)-$CaSO_3$ system experimental group, so the degradation of As(III) was due to the conversion to As(V) by oxidation reaction. The deployment of Fe(III) or $CaSO_3$ alone led to 20% degradation of As(III) in 1 h, which is in obvious contrast to the combination of Fe(III) and $CaSO_3$ (72%).

Fe(III) in the solution mainly existed in the form of colloid at near-neutral pH and thus adsorbed As(III) through surface complexation. As(III) can then be oxidized by electron transfer from As(III) to Fe(III) induced by radiation absorption via ligand-to-metal charge transfer [28]. The decrease in As(III) concentration in the presence of Fe(III) in the absence of sulfite may be due to radical oxidation pathway of As(III) and adsorption on colloidal ferric hydroxides followed by oxidation [19]. The decrease in As(III) concentration in the presence of sulfite alone may be due to the auto-oxidation reaction of SO_3^{2-} on the surface of $CaSO_3$ solid surface (>Ca(II)-SO_3^{2-} in Equations (9)–(13)) and the co-oxidation of SO_3^{2-} with As (III) under alkaline conditions on the surface of the $CaSO_3$ solid (Equations (14) and (15)).

$$>CaSO_3 \rightarrow >Ca(II)\text{-}SO_3^{2-} \quad (9)$$

$$>Ca(II)\text{-}SO_3^{2-} + O_2 \rightarrow >Ca(II)\text{-}SO_3^{2-}\text{-}O_2 \quad (10)$$

$$>Ca(II)\text{-}SO_3^{2-}\text{-}O_2 \rightarrow >Ca(II)\text{-}SO_3^{\bullet-} + O_2^{\bullet-} \quad (11)$$

$$>Ca(II)\text{-}SO_3^{\bullet-} + O_2 \rightarrow >Ca(II)\text{-}SO_5^{\bullet-} \quad (12)$$

$$>Ca(II)\text{-}SO_5^{\bullet-} + As(III) \rightarrow >Ca(II)\text{-}As(V) + SO_4^{2-} \quad (13)$$

$$>CaSO_3 + H_2O \rightarrow >Ca(II)\text{-}OH^- + SO_3^{2-} + H^+ \quad (14)$$

$$>Ca(II)\text{-}OH^- \text{ (mediated reaction): } SO_3^{2-} + As(III) + O_2 \rightarrow SO_4^{2-} + As(V) \quad (15)$$

When Fe(III) and $CaSO_3$ solid powders were added simultaneously, the reaction rate of the system increased rapidly. This is basically consistent with the previous research results

on the Fe(III)-sulfite system [14,20,21], suggesting that the activation of SO_3^{2-} may occur either in the liquid phase or on the surface of $CaSO_3$ particles (Equations (16) and (17)). Considering that irons can easily form hydroxide precipitates at near neutral pH and aggregate with $CaSO_3$ to form composite particles, the activation of SO_3^{2-} on the solid surface may also be important.

$$>Ca(II)\text{-}SO_3^{2-} + Fe(III) \rightarrow >Ca(II)\text{-}SO_3^{2-}\text{-}Fe(III) \quad (16)$$

$$>Ca(II)\text{-}SO_3^{2-}\text{-}Fe(III) \rightarrow >Ca(II)\text{-}SO_3^{\bullet-} + Fe(II) \quad (17)$$

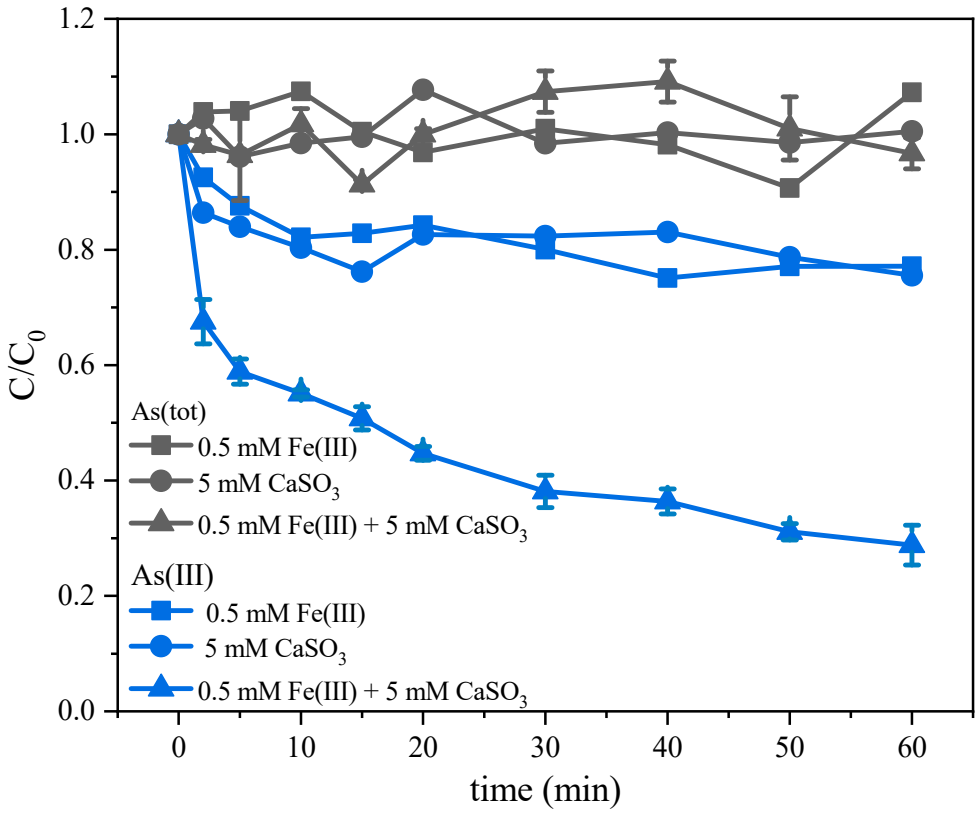

Figure 1. Concentration changes of As(III) and As(tot) in the control experiments of Fe(III)-$CaSO_3$ system. Initial conditions: [Fe(III)] = 0.5 mM, [$CaSO_3$] = 5 mM, [As(III)] = 5 μM, pH 6.0, air bubbling at 0.5 L min^{-1}.

2.2. Effects of Fe(III) and $CaSO_3$ Dosages on As(III) Oxidation

The effects of Fe(III) and $CaSO_3$ dosages on As(III) oxidation were investigated (Figure 2). For optimizing Fe(III) dosage, 0.5 mM Fe(III) achieved the best As(III) oxidation. When Fe(III) concentrations exceed this value, As(III) oxidation was conversely inhibited. This can be explained by the fact that a greater amount of $Fe(OH)_3$ colloid might be produced in the reaction system, which would inhibit the dissolution and release of $CaSO_3$ and the activation ability of Fe(III) towards HSO_3^-. Besides, a large amount of Fe(II) generated by the initial reactions (Equations (1)–(3)) could also consume $SO_5^{\bullet-}/SO_4^{\bullet-}$ in the solution (Equations (18) and (19)). However, due to the presence of excess $CaSO_3$, HSO_3^- continues to slowly dissolve, and the oxidation efficiency of As(III) does not decrease steadily with the increase in Fe(III) concentration. Hence, Fe(III) concentration should not be the only limiting factor for As(III) oxidation in the Fe(III)-$CaSO_3$ system.

$$SO_5^{\bullet-} + Fe^{2+} + H^+ \rightarrow HSO_5^- + Fe^{3+} \quad (18)$$

$$SO_4^{\bullet-} + Fe^{2+} \rightarrow SO_4^{2-} + Fe^{3+} \quad (19)$$

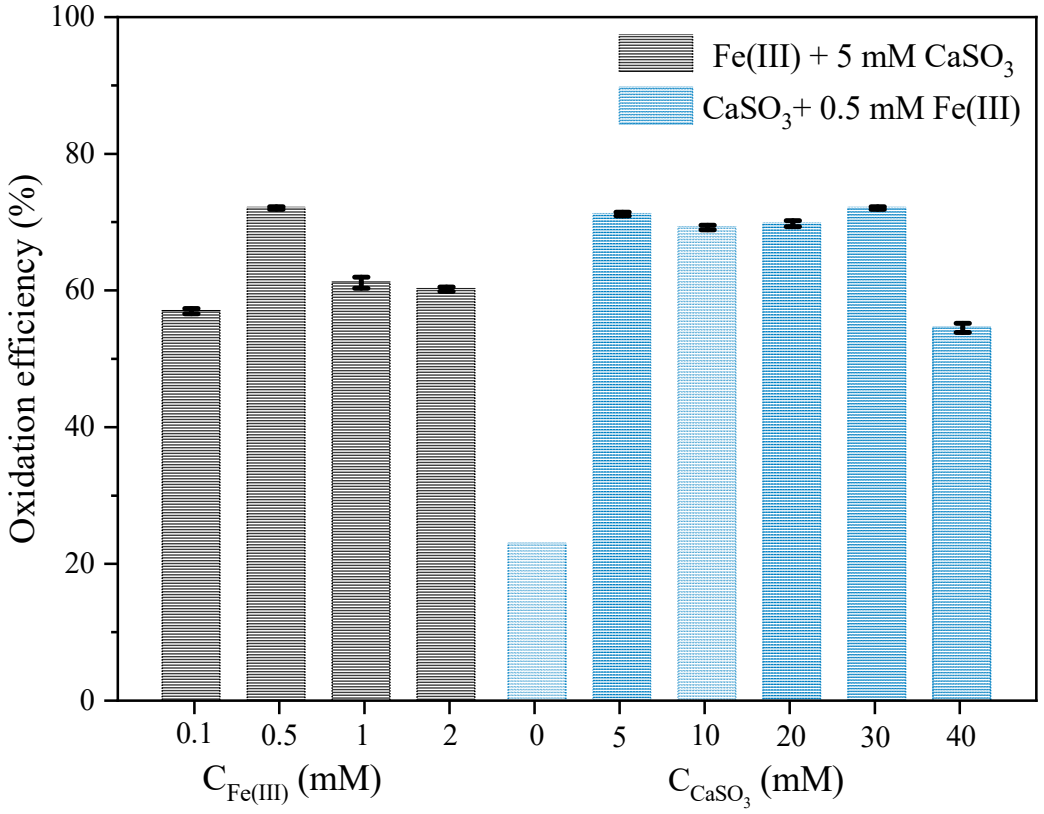

Figure 2. Effect of dosage of Fe(III)/$CaSO_3$ on the oxidation efficiency of As(III) in the Fe(III)-$CaSO_3$ system after a reaction time of 60 min. Initial conditions: [As(III)] = 5 μM, pH 6.0, air bubbling at 0.5 L min^{-1}. Fe(III) + 5 mM $CaSO_3$: [Fe(III)] = 0.1–2.0 mM, [$CaSO_3$] = 5 mM; $CaSO_3$ + 0.5 mM Fe(III): [Fe(III)] = 0.5 mM, [$CaSO_3$] = 0–40 mM.

Meanwhile, for optimizing $CaSO_3$ dosages, 30 mM $CaSO_3$ achieved the best As(III) oxidation. When $CaSO_3$ concentration exceed this value, the concentration of S(IV) is much higher than that of As(III) in the solution and As(III) oxidation was inhibited. The reasons for the inhibition of As(III) oxidation may be that S(IV) on the surface of $CaSO_3$ may compete with As(III) for $SO_4^{\bullet-}$ [Equation (20)]. Therefore, the removal of $SO_4^{\bullet-}$ by excess S(IV) may be a reason for the inhibition of As(III) oxidation. Zhou et al. [18] delineated the reactions of $SO_5^{\bullet-}/SO_4^{\bullet-}$ in the Fe(III)–S(IV) system, indicating that an excess of S(IV) or Fe(II) may inhibit the reactions of $SO_5^{\bullet-}/SO_4^{\bullet-}$. At the same time, excess $CaSO_3$ may lead to a large number of particles around Fe(III), which would inactivate it and reduce its ability to activate S(IV).

$$SO_4^{\bullet-} + HSO_3^- \rightarrow HSO_4^- + SO_3^{\bullet-} \quad (20)$$

2.3. Effect of pH on As(III) Oxidation

To investigate the effect of pH on the Fe(III)-$CaSO_3$ system, experiments were conducted at pH 4, 6, 8, and 10 (Figure 3). It was found that As(III) oxidation efficiency varied from 63% at pH 10 to 80% at pH 4 within 60 min and when at pH 6 and 7, the efficiency of the system had no obvious difference, reaching about 75%.

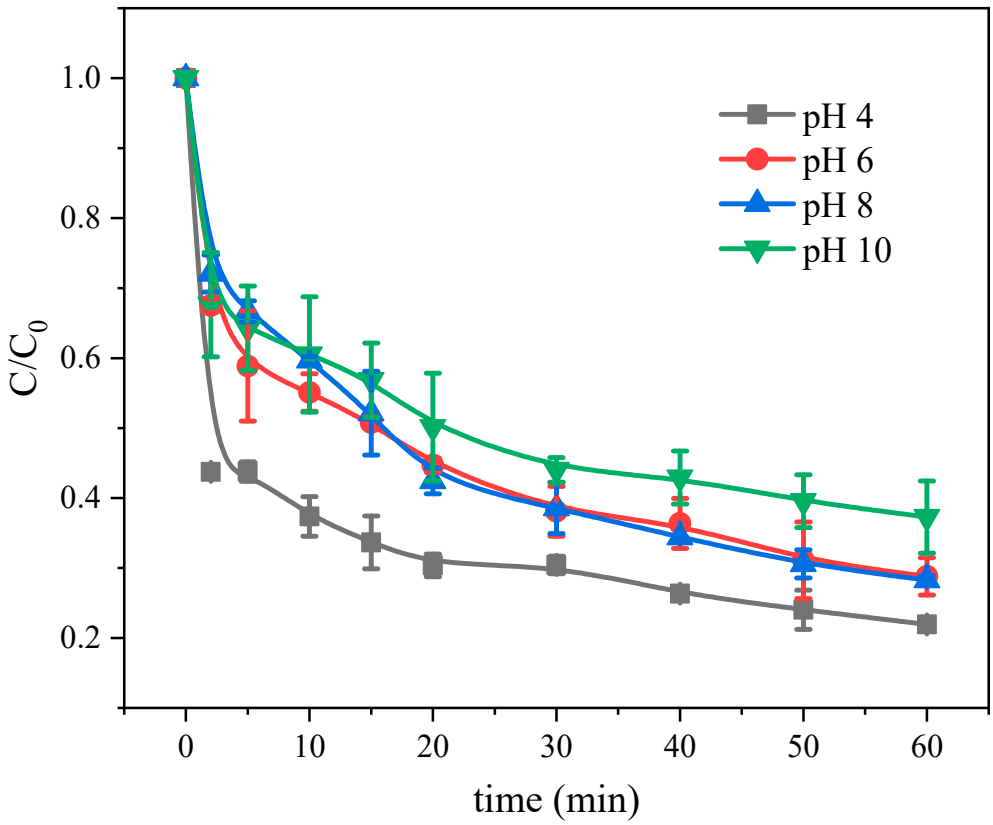

Figure 3. Effect of pH on the Fe(III)-$CaSO_3$ system. Initial conditions: [Fe(III)] = 0.5 mM, [$CaSO_3$] = 5 mM, [As(III)] = 5 μM, air bubbling at 0.5 L min^{-1}.

Lower pH values led to more efficient As(III) oxidation, consistent with conclusions drawn for the Fe(III)-Na_2SO_3 system [12]. This may be because, at near-neutral pH, the Fe in the solution mainly exists in the form of $Fe(OH)_2^+$ or $Fe(OH)_3$, and forms a complex with sulfite [19]. Fe(III) and Fe(II) in the reaction solution can be rapidly converted, according to Equations (3) and (7), which is also a key step affecting the reaction rate in the Fe(III)-Na_2SO_3 system. When the pH approaches alkaline, the system still maintained good oxidation efficiency, probably because the interconversion of $SO_4^{\bullet-}$ to $HO^{\bullet}$ (Equation (21)) is favored at pH > 8.5 and the direct activation of sulfite by alkalion [29].

$$SO_4^{\bullet-} + OH^- \rightarrow SO_4^{2-} + HO^{\bullet} \text{ (alkaline pH)} \quad (21)$$

2.4. Effect of the Initial Concentration of As(III) on Its Oxidation

As(III) oxidation processes followed Langmuir–Hinshelwood (L–H) kinetics (Equation (22) [30].

$$r_0 = \frac{K_{L-H} \times K \times C_0}{1 + K_{L-H} \times C_0} \quad (22)$$

The kinetics of As(III) oxidation in the Fe(III)-$CaSO_3$ system was studied by the initial rate method. The initial rate r_0 was taken as the average value of the change of As(III) concentration over the initial period. The initial oxidation rate of As(III) increased with its initial concentration (Figure 4). When the initial As(III) concentration is higher, the As(III) oxidation rate continues to increase. The relationship between r_0 and C_0 for As(III) oxidation followed the Langmuir–Hinshelwood (L-H) equation of heterogeneous reaction kinetics with a low adsorption constant (K) of 0.07 μM^{-1} (Table 1). Therefore, $K \times C_0$ in the denominator can be ignored in the realm of low concentrations. The L-H equation thus becomes a simple pseudo-first-order linear kinetic equation ($r_0 = k_{L-H} \times K \times C_0 = 0.3\ C_0$,

μM min^{-1}), which indicates the involvement of a solid-phase interface reaction mechanism in the oxidation of As(III) in the Fe(III)-$CaSO_3$ system.

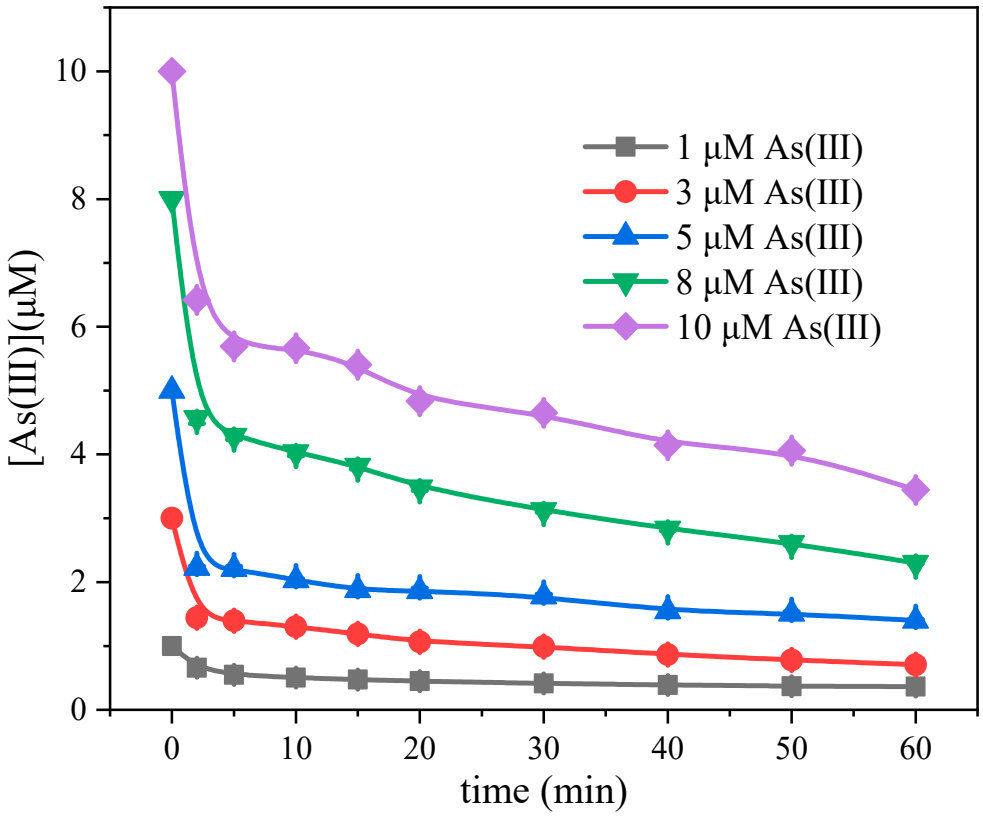

Figure 4. Effect of initial As(III) concentration on the Fe(III)-$CaSO_3$ system. Initial conditions: [Fe(III)] = 0.5 mM, [$CaSO_3$] = 30 mM, [As(III)] = 1–10 μM, pH 6.0, air bubbling at 0.5 L min^{-1}.

Table 1. Oxidation kinetics of As(III) according to the L-H equation in the Fe(III)-$CaSO_3$ system.

C_0	r_0	Kinetic Equation	k_{L-H}	K	R^2
1	0.1694	$r_0 = \frac{0.3282c}{(1+0.07382c)}$	4.446	0.074	0.972
3	0.6731				
5	1.3876				
8	1.7167				
10	1.7896				

C_0 is initial concentration (μM); r_0 initial rate (μM min^{-1}), k_{L-H} the rate constant (μM min^{-1}), and K the adsorption constan (μM min^{-1}).

2.5. Contribution of Free Radicals to As(III) Oxidation

Several studies have shown that the generation of reactive oxygen species is the main reason for the oxidative degradation of pollutants in acidic environments [31,32]. The Fe(III)-$CaSO_3$ system involves oxysulfur free radicals, including $SO_3^{\bullet-}$, $SO_5^{\bullet-}$, and $SO_4^{\bullet-}$, formed according to Equations (1)–(8). $HO^{\bullet}$ may be generated from $SO_4^{\bullet-}$, according to Equations (21) and (23), and may also contribute to the degradation of As(III). Quenching experiments were performed to better understand the reaction mechanisms (Figure 5). Ethanol (EtOH) and tert-butyl alcohol (TBA) were employed as radical scavengers.

$$SO_4^{\bullet-} + H_2O \rightarrow SO_4^{2-} + HO^{\bullet} + H^+ \quad (23)$$

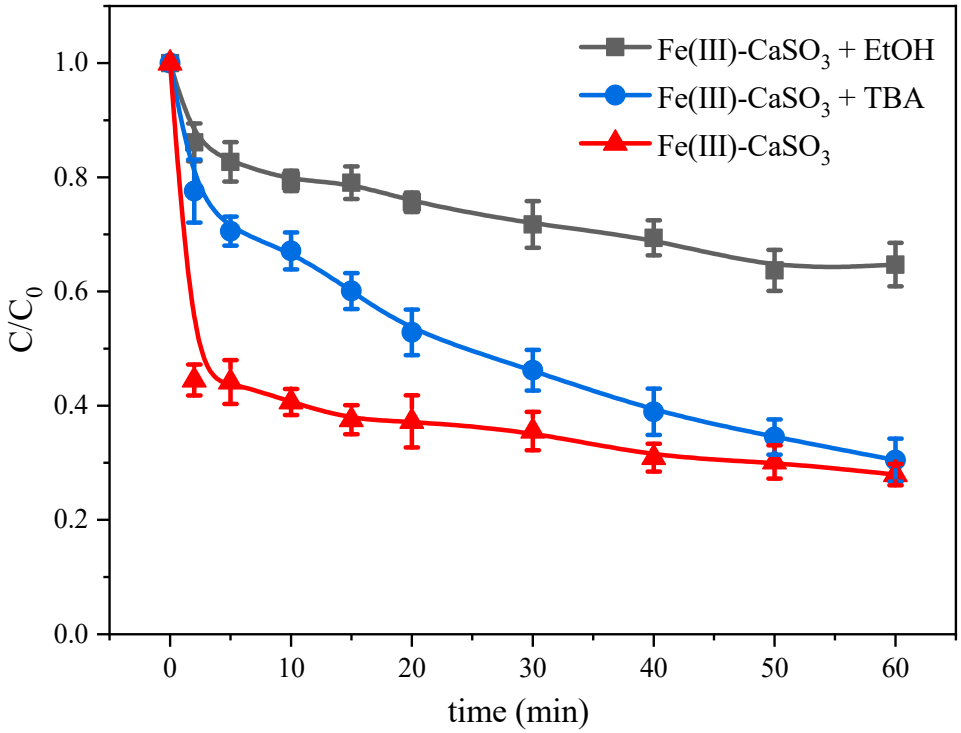

Figure 5. Contribution of free radicals in the Fe(III)-$CaSO_3$ system. Initial conditions: [Fe(III)] = 0.5 mM, [$CaSO_3$] = 30 mM, [As(III)] = 5 μM, [EtOH] = 5 mM, [TBA] = 2 mM, pH 6.0, air at 0.5 L min^{-1}.

EtOH has similar rate constants for $SO_4^{\bullet-}$ and $HO^{\bullet}$ ($k_{EtOH,HO}^{\bullet}$ = (1.8–2.8) × 10^9 M^{-1} s^{-1}, $k_{EtOH,SO4}^{\bullet-}$ = (1.6–7.7) × 10^7 M^{-1} s^{-1}) [33]. However, the rate constant for the reaction between TBA and $HO^{\bullet}$ ($k_{TBA,HO}^{\bullet}$ = (3.8–7.6) × 10^8 L mol^{-1} s^{-1}) is 1000-times higher than that for the reaction between TBA and $SO_4^{\bullet-}$ ($k_{TBA,SO4}^{\bullet-}$ = (4.0–9.1) × 10^5 L mol^{-1} s^{-1}) [34]. Hence, $SO_4^{\bullet-}$ and $HO^{\bullet}$ contributions for As(III) oxidation can be distinguished by adding EtOH and TBA, respectively. After adding EtOH (5 mM), it was found that the oxidation rate of As(III) decreased from 0.4 to 0.07 min^{-1}, implying that this main reactive species generated by Fe(III)-$CaSO_3$ process were attributable to $SO_4^{\bullet-}$ and $HO^{\bullet}$, the residual should be caused by $SO_5^{\bullet-}$, as $SO_3^{\bullet-}$ possesses so weak oxidative ability that cannot oxidize As(III) and $SO_3^{\bullet-}$ tends to be rapidly oxidized to $SO_5^{\bullet-}$ in the oxygen-containing condition [28]. Therefore, we surmised that $SO_5^{\bullet-}$ caused the 17.5% As(III) oxidation. Moreover, when adding TBA (2 mM) into the solution, the oxidative rate decreased to 0.13 min^{-1}, showing that $HO^{\bullet}$ was responsible for about 67.5% of the As(III) oxidation. In conclusion, the reactive species mainly responsible in the Fe(III)-$CaSO_3$ system involved $SO_4^{\bullet-}$, $HO^{\bullet}$ and $SO_5^{\bullet-}$ generation that accounted for 15%, 67.5% and 17.5% contribution for As(III)oxidation, respectively.

3. Materials and Methods

3.1. Materials

$NaAsO_2$ (99.5%; Gracia Chemical Technology Co., Ltd., Chengdu, China) was dried in a desiccator for 24 h prior to use. $Na_2HAsO_4{\cdot}7H_2O$ was purchased from Alfa Aesar (A Johnson Matthey Co., Ltd., Shanghai, China). $CaSO_3$ was purchased from Shanghai Aladdin Bio-Chem Technology Co., Ltd. (Shanghai, China). $Fe_2(SO4)_3$, NaOH, H_2SO_4, KBH_4 and HCl were purchased from Sinopharm Chemical Reagent Co., Ltd. (Shanghai, China). Ethanol (EtOH) and tert-butyl alcohol (TBA) were used for radical quenching. All chemicals were of analytical reagent grade or higher purity, and were used without further purification.

3.2. Reaction Procedure

All experiments were performed in a 250 mL cylindrical reactor cooled by external jacket water circulation at a constant temperature of 25 °C (Figure 6). A 250 mL solution containing As(III) at the desired concentration was placed in the reactor and constantly stirred with a polytetrafluoroethylene-coated magnetic stirrer. Sulfite consumed oxygen quickly in aqueous solution, so hence synthetic air was constantly pumped into the reaction solution. Then, Fe(III) and $CaSO_3$ solutions were added, and the pH was quickly re-adjusted to the desired value (± 0.1). Aliquots (4.5 mL) were withdrawn at specific time intervals and immediately mixed with 0.5 mL portions of 6 M HCl. The resultant mixtures were filtered through a 0.22 μm filter and preserved in the dark at low temperature (4 °C) for less than 4 h before analysis. The concentrations of As(III) and As(V) in the filtrates were determined by HPLC-HG-AFS.

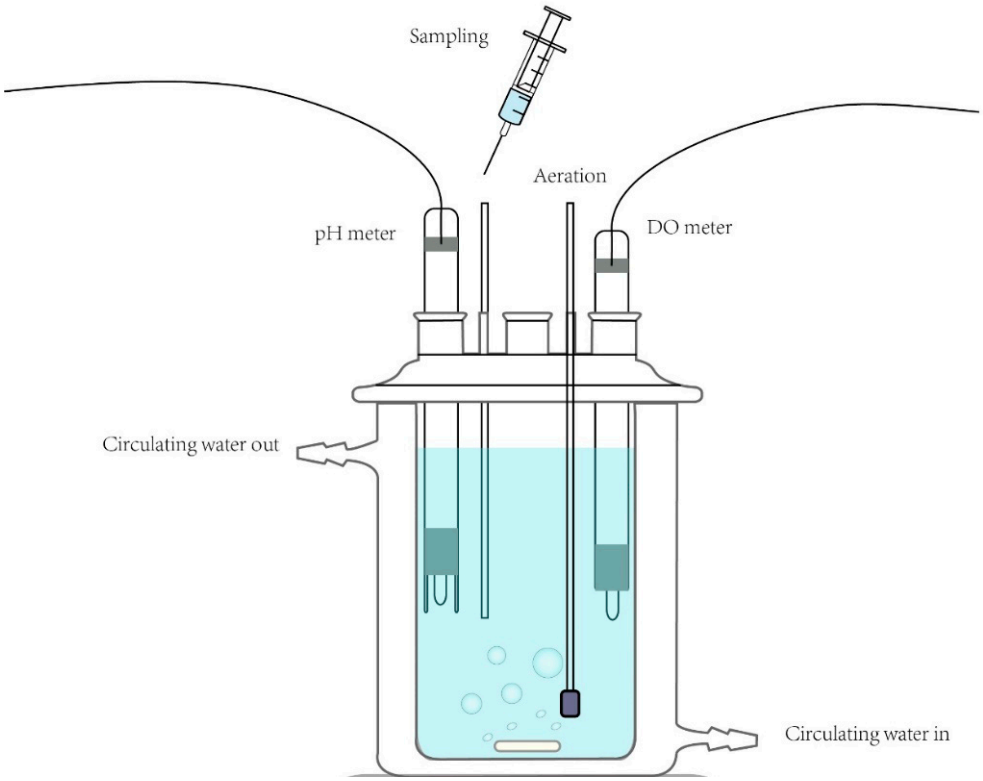

Figure 6. Schematic of experimental setup.

3.3. Analysis

The sample was acidified and filtered in advance, so that the adsorbed As in the reaction solution has basically transformed it into dissociative state. Arsenic concentration was determined by using liquid-phase hydride-generation–atomic fluorescence spectrometry (LC-HG-AFS). As(III) and As(V) in the reaction solution were separated on an ion chromatography column (PRP-X100, Hamilton, Switzerland) by eluting with a phosphate mobile phase (45 mM, pH 5.6). The concentrations of As(III) and As(V) were determined using 5% HCl–2% KBH_4 solution in HG-AFS [29].

4. Conclusions

The Fe(III)-$CaSO_3$ system can generate free radicals and effectively degrade As(III). It has been demonstrated that hydroxyl and oxysulfur radicals are the active species in the mechanism of As(III) oxidation. Under conditions of pH 6.0, the optimal concentrations of Fe(III) and $CaSO_3$ in the Fe(III)-$CaSO_3$ system are 0.5 and 30 mM, respectively, whereupon the As(III) oxidation efficiency can reach 72.1% after 1 h. Radical scavenging tests have

indicated that oxidation of As(III) is caused by $HO^{\bullet}$ (67.5%), $SO_5^{\bullet-}$ (17.5%) and $SO_4^{\bullet-}$ (15%). The results presented here imply that in the Fe(III)-$CaSO_3$ system, replacing soluble sulfites with slightly soluble sulfites is an effective strategy in oxidizing As(III) to As(V), and in the Fe(III)-$CaSO_3$ system, replacing soluble sulfites with slightly soluble sulfites is an effective in degrading arsenic, and the Fe(III)-$CaSO_3$ system offers a cost-effective process for arsenic removal from contaminated waters, and that sulfite holds significant promise as a new resource utilization method of desulfurized gypsum.

Author Contributions: M.C., and S.Q. performed the As(III) oxidation experiments; F.W. and G.M. conceived and designed the experiments; J.L. and S.Q. analyzed the data; M.C. and S.Q. participated in drafting the article; all authors revised the article. All authors have read and agreed to the published version of the manuscript.

Funding: The WOW program of the CAP 20-25 project (UCA).

Data Availability Statement: Data is contained within the article.

Acknowledgments: This work was financially supported by the Laboratoire International Associé (LIA) entre l'Université Clermont Auvergne (UCA) et l'Université de Wuhan (WHU), the WOW program of the CAP 20-25 project (UCA).

Conflicts of Interest: The authors declare no conflict of interest.

Sample Availability: The materials used in the study are commercially available and can be purchased from the relevant firms.

References

1. Renew, J.E.; Huang, C.; Burns, S.E.; Carrasquillo, M.; Sun, W.; Ellison, K.M. Immobilization of heavy metals by solidification/stabilization of Co-disposed flue gas desulfurization brine and coal fly ash. *Energy Fuels* **2016**, *30*, 5042–5051. [CrossRef]
2. Song, W.; Zhou, J.; Wang, B.; Li, S.; Cheng, R. Production of SO_2 gas: New and efficient utilization of flue gas desulfurization gypsum and pyrite resources. *Ind. Eng. Chem. Res.* **2019**, *58*, 20450–20460. [CrossRef]
3. Chi, C.; Zhao, C.; Sun, X.; Wang, Z. Reclamation of saline-sodic soil properties and improvement of rice (*Oriza sativa* L.) growth and yield using desulfurized gypsum in the west of Songnen Plain, northeast China. *Geoderma* **2012**, *187*, 24–30. [CrossRef]
4. Lee, Y.B.; Bigham, J.M.; Dick, W.A.; Kim, P.J. Impact of flue gas desulfurization-calcium sulfite and gypsum on soil microbial activity and wheat growth. *Soil Sci.* **2008**, *173*, 534–543. [CrossRef]
5. Nan, J.; Chen, X.; Chen, C.; Lashari, M.S.; Deng, J.; Du, Z. Impact of flue gas desulfurization gypsum and lignite humic acid application on soil organic matter and physical properties of a saline-sodic farmland soil in Eastern China. *J. Soil Sediments* **2016**, *16*, 2175–2185. [CrossRef]
6. Yang, P.; Li, X.; Tong, Z.; Li, Q.; He, B.; Wang, L.; Guo, S.; Xu, Z. Use of flue gas desulfurization gypsum for leaching Cd and Pb in reclaimed tidal flat soil. *Environ. Sci. Pollut. Res.* **2016**, *23*, 7840–7848. [CrossRef]
7. Schomberg, H.H.; Endale, D.M.; Jenkins, M.B.; Chaney, R.L.; Franklin, D.H. Metals in soil and runoff from a piedmont hay field amended with broiler litter and flue gas desulfurization gypsum. *J. Environ. Qual.* **2018**, *47*, 326–335. [CrossRef]
8. Vaclavikova, M.; Gallios, G.; Hredzak, S.; Jakabsky, S. Removal of arsenic from water streams: An overview of available techniques. *Clean Technol. Environ. Policy.* **2008**, *10*, 89–95. [CrossRef]
9. Wang, S.; Zhou, N. Removal of carbamazepine from aqueous solution using sono-activated persulfate process. *Ultrason. Sonochem.* **2016**, *29*, 156–162. [CrossRef] [PubMed]
10. Shi, P.; Su, R.; Wan, F.; Zhu, M.; Li, D.; Xu, S. Co_3O_4 nanocrystals on graphene oxide as a synergistic catalyst for degradation of Orange II in water by advanced oxidation technology based on sulfate radicals. *Appl. Catal. B* **2012**, *123*, 265–272. [CrossRef]
11. Zhou, D.; Chen, L.; Zhang, C.; Yu, Y.; Zhang, L.; Wu, F. A novel photochemical system of ferrous sulfite complex: Kinetics and mechanisms of rapid decolorization of Acid Orange 7 in aqueous solutions. *Water Res.* **2014**, *57*, 87–95. [CrossRef]
12. Chen, L.; Peng, X.; Liu, J.; Li, J.; Wu, F. Decolorization of orange II in aqueous solution by an Fe(II)/sulfite system: Replacement of persulfate. *Ind. Eng. Chem. Res.* **2012**, *51*, 13632–13638. [CrossRef]
13. Guo, Y.; Lou, X.; Fang, C.; Xiao, D.; Wang, Z.; Liu, J. Novel photo-sulfite system: Toward simultaneous transformations of inorganic and organic pollutants. *Environ. Sci. Technol.* **2013**, *47*, 11174–11181. [CrossRef]
14. Zhang, L.; Chen, L.; Xiao, M.; Zhang, L.; Wu, F.; Ge, L. Enhanced decolorization of orange II solutions by the Fe(II)–sulfite system under xenon lamp irradiation. *Ind. Eng. Chem. Res.* **2013**, *52*, 10089–10094. [CrossRef]
15. Zhou, D.; Yuan, Y.; Yang, S.; Gao, H.; Chen, L. Roles of oxysulfur radicals in the oxidation of acid orange 7 in the Fe(III)–sulfite system. *J. Sulfur Chem.* **2015**, *36*, 373–384. [CrossRef]
16. Zhou, D.; Chen, L.; Li, J.; Wu, F. Transition metal catalyzed sulfite auto-oxidation systems for oxidative decontamination in waters: A state-of-the-art minireview. *Chem. Eng. Sci.* **2018**, *346*, 726–738. [CrossRef]

17. Bavasso, I.; Vilardi, G.; Stoller, M.; Chianese, A.; Di Palma, L. Perspectives in Nanotechnology Based Innovative Applications for The Environment. *Chem. Eng. Trans.* **2016**, *47*, 55–60.
18. Di Palma, L.; Verdone, N.; Vilardi, G. Kinetic Modeling of Cr(VI) Reduction by nZVI in Soil: The Influence of Organic Matter and Manganese Oxide. *Bull. Environ. Contam. Toxicol.* **2018**, *101*, 692–697. [CrossRef]
19. Xu, J.; Ding, W.; Wu, F.; Mailhot, G.; Zhou, D.; Hanna, K. Rapid catalytic oxidation of arsenite to arsenate in an iron(III)/sulfite system under visible light. *Appl. Catal. B* **2016**, *186*, 56–61. [CrossRef]
20. Chen, L.; Tang, M.; Chen, C.; Chen, M.; Luo, K.; Xu, J.; Wu, F. Efficient bacterial inactivation by transition metal catalyzed auto-oxidation of sulfite. *Environ. Sci. Technol.* **2017**, *51*, 12663–12671. [CrossRef]
21. Yuan, Y.; Luo, T.; Xu, J.; Li, J.; Wu, F. Enhanced oxidation of aniline using Fe(III)-S(IV) system: Role of different oxysulfur radicals. *Chem. Eng. J.* **2019**, *362*, 183–189. [CrossRef]
22. Lee, Y.J.; Rochelle, G.T. Oxidative degradation of organic acid conjugated with sulfite oxidation in flue gas desulfurization: Products, kinetics, and mechanism. *Environ. Sci. Technol.* **1987**, *21*, 266–272. [CrossRef]
23. Neta, P.; Robert, E.H.; Ross, A.B. Rate constants for reactions of inorganic radicals in aqueous solution. *J. Phys. Chem. Ref. Data.* **1988**, *17*, 1027–1284. [CrossRef]
24. Lente, G.; Fábián, I. Kinetics and mechanism of the oxidation of sulfur(IV) by iron(III) at metal ion excess. *J. Chem. Soc. Dalton Trans.* **2002**, *5*, 778–784. [CrossRef]
25. Zhang, Y.; Zhou, J.; Li, C.; Guo, S.; Wang, G. Reaction kinetics and mechanism of Iron(II)-induced catalytic oxidation of sulfur(IV) during wet desulfurization. *Ind. Eng. Chem. Res.* **2012**, *51*, 1158–1165. [CrossRef]
26. Ge, J.; Zhou, Y.; Yang, Y.; Xue, M. Catalytic oxidative desulfurization of gasoline using Ionic liquid emulsion system. *Ind. Eng. Chem. Res.* **2012**, *50*, 13686–13692. [CrossRef]
27. Shao, B.; Dong, H.; Sun, B.; Guan, X. Role of ferrate(IV) and ferrate(V) in activating ferrate(VI) by calcium sulfite for enhanced oxidation of organic contaminants. *Environ. Sci. Technol.* **2019**, *53*, 894–902. [CrossRef]
28. Luo, T.; Peng, Y.; Chen, L.; Li, J.; Wu, F.; Zhou, D. Metal-Free Electro-activated sulfite process for As(III) oxidation in water using graphite electrodes. *Env. Sci. Technol.* **2020**, *54*, 10261–11026. [CrossRef]
29. Xu, J.; Li, J.; Wu, F.; Zhang, Y. Rapid photooxidation of As(III) through surface complexation with nascent colloidal ferric hydroxide. *Environ. Sci. Technol.* **2014**, *48*, 272–278. [CrossRef]
30. Nguyen, T.V.; Vigneswaran, S.; Ngo, H.H.; Kandasamy, J.; Choi, H.C. Arsenic removal by photo-catalysis hybrid system. *Sep. Purif. Technol.* **2008**, *61*, 44–50. [CrossRef]
31. Patrick, M.; Jaromir, J.; Michèle, B. Degradation of diuron photoinduced by iron(III) in aqueous solution. *Pesticide Sci.* **1997**, *49*, 259–267.
32. Qu, P.; Zhao, J.; Shen, T.; Hidaka, H. TiO_2-assisted photodegradation of dyes: A study of two competitive primary processes in the degradation of RB in an aqueous TiO_2 colloidal solution. *J. Mol. Catal. A Chem.* **1998**, *129*, 257–268. [CrossRef]
33. Mclachlan, G.A.; Muller, J.G.; Rokita, S.E.; Burrows, C.J. Metal-mediated oxidation of guanines in DNA and RNA: A comparison of cobalt(II), nickel(II) and copper(II) complexes. *Inorganica Chimica Acta.* **1996**, *251*, 193–199. [CrossRef]
34. Anipsitakis, G.P.; Dionysiou, D.D. Radical generation by the interaction of transition metals with common oxidants. *Environ. Sci. Technol.* **2004**, *38*, 3705–3712. [CrossRef]